The Journal of Infectious Diseases

SUPPLEMENT ARTICLE

Resistance of Cynomolgus Monkeys to Nipah and Hendra Virus Disease Is Associated With Cell-Mediated and Humoral Immunity

Abhishek N. Prasad,[1,2,†] Courtney Woolsey,[1,2,†] Joan B. Geisbert,[1,2] Krystle N. Agans,[1,2] Viktoriya Borisevich,[1,2] Daniel J. Deer,[1,2] Chad E. Mire,[1,2] Robert W. Cross,[1,2] Karla A. Fenton,[1,2] Christopher C. Broder,[3] and Thomas W. Geisbert[1,2]

[1]Galveston National Laboratory and [2]Department of Microbiology and Immunology, University of Texas Medical Branch, Galveston, [3]Department of Microbiology and Immunology, Uniformed Services University, Bethesda, Maryland

Background. The henipaviruses, Hendra virus (HeV) and Nipah virus (NiV), are capable of causing severe and often lethal respiratory and/or neurologic disease in animals and humans. Given the sporadic nature of henipavirus outbreaks, licensure of vaccines and therapeutics for human use will likely require demonstration of efficacy in animal models that faithfully reproduce the human condition. Currently, the African green monkey (AGM) best mimics human henipavirus-induced disease.

Methods. The pathogenic potential of HeV and both strains of NiV (Malaysia, Bangladesh) was assessed in cynomolgus monkeys and compared with henipavirus-infected historical control AGMs. Multiplex gene and protein expression assays were used to compare host responses.

Results. In contrast to AGMs, in which henipaviruses cause severe and usually lethal disease, HeV and NiVs caused only mild or asymptomatic infections in macaques. All henipaviruses replicated in macaques with similar kinetics as in AGMs. Infection in macaques was associated with activation and predicted recruitment of cytotoxic $CD8^+$ T cells, Th1 cells, IgM^+ B cells, and plasma cells. Conversely, fatal outcome in AGMs was associated with aberrant innate immune signaling, complement dysregulation, Th2 skewing, and increased secretion of MCP-1.

Conclusion. The restriction factors identified in macaques can be harnessed for development of effective countermeasures against henipavirus disease.

Keywords. Nipah virus; Hendra virus; henipavirus; paramyxovirus; primate; pathogenesis; animal model; transcriptomics; cytokines; chemokines.

Hendra virus (HeV) and Nipah virus (NiV) are zoonotic RNA viruses in the genus *Henipavirus* (family *Paramyxoviridae*) and cause disease outbreaks in livestock and humans [1, 2]. The main pathological features of HeV and NiV infection in people and several species of mammals are severe systemic respiratory and/or neurologic disease [3]. Several species of pteropid fruit bats serve as reservoirs for HeV and NiV [4]. HeV is endemic to Australia and causes sporadic outbreaks in equines with rare instances of subsequent infections in humans [5]. Currently, 2 phylogenetically distinct strains of NiV have been identified: the Malaysia strain (NiV_M), which caused the initial outbreak of NiV in Malaysia and Singapore [6], and the Bangladesh strain (NiV_B), which is responsible for nearly annual outbreaks in Bangladesh and India [7]. The case fatality rate (CFR) in humans for both HeV and NiV has ranged from ~ 40 to 75% [5, 8–10], although a recent outbreak of NiV_B in India resulted in 21 deaths among 23 total cases (91% CFR) [11]. A number of studies reporting human-to-human transmission also points to the potential of NiV as a pandemic threat [12–14].

Currently, there are no vaccines or treatments against HeV or NiV licensed for human use. Licensure of any medical countermeasure may require demonstration of efficacy in an animal model(s) of henipavirus infection [15]. Mice, guinea pigs, hamsters, cats, ferrets, and non-human primates (NHPs) have been evaluated as animal models of human henipavirus infection and disease [16]. Of these, the African green monkey (*Chlorocebus aethiops*; AGM) appears to best reflect HeV and NiV infection in humans. Henipavirus-infected AGMs exhibit severe respiratory pathology, neurological disease, and generalized vasculitis [17–26].

Although AGMs ostensibly excel as a model of human henipavirus infection, the ability to use different NHP species, particularly cynomolgus (*Macaca fascicularis*) and rhesus macaques (*Macaca mulatta*), presents a number of advantages. Cynomolgus and rhesus macaques are the most commonly used NHPs for biomedical research in the United States [27];

[†]These authors contributed equally.

Correspondence: Thomas W. Geisbert, PhD, University of Texas Medical Branch at Galveston, Galveston National Laboratory, 301 University Blvd, Galveston, TX 77550-0610 (twgeisbe@utmb.edu).

The Journal of Infectious Diseases® 2020;221(S4):S436–47

DOI: 10.1093/infdis/jiz613

therefore, a larger supply of animals is available. There is also more information regarding important considerations, such as cross-reactivity with human reagents. Finally, as HeV and NiV must be contained in biosafety level (BSL)-4 facilities, a number of logistical considerations pertaining to NHP housing would make working with these species more favorable. Specifically, AGMs can be persistently infected with viruses, such as simian immunodeficiency virus (SIV) and simian hemorrhagic fever virus (SHFV), which cause lethal infection if transmitted to macaques [28, 29]. Accordingly, AGMs should not be housed in the same area as macaques. Moreover, space is often limited in biocontainment. Most viruses used in BSL-4 facilities, including Ebola, Marburg, Lassa, Junin, and Crimean-Congo hemorrhagic fever viruses, all employ cynomolgus and/or rhesus macaques as preferred NHP models. Thus, there are important conveniences in using macaques as a henipavirus disease model.

Here we assessed the pathogenic potential of HeV, NiV_B, and NiV_M in cynomolgus macaques. We compared our findings using historical data from HeV- and NiV-infected AGMs. Surprisingly, we found that although macaques sustained virus replication to similar levels as AGMs, these animals failed to develop the fatal clinical illness typically observed in AGMs. Our data provide insight into the intra- and interspecies restriction factors of lethal henipavirus infection.

METHODS

Viruses

A detailed description of the viruses used in this study is available in the Supplementary Methods.

Animal Infection

A detailed description of henipavirus challenge of AGMs and cynomolgus macaques is available in the Supplementary Methods.

Ethics Approval and Consent to Participate

The animal studies were performed at the Galveston National Laboratory, University of Texas Medical Branch at Galveston (UTMB), and were approved by the UTMB Institutional Animal Care and Use Committee. This facility is fully accredited by the Association for Assessment and Accreditation of Laboratory Animal Care International.

Detection of Virus from NiV_B-Infected AGMs

RNA was isolated from blood or tissues and assessed using primers/probe targeting the N gene as described previously [20] and [21] and detailed in the Supplementary Methods.

Clinical Pathology and Host Immune Response

Hematology, clinical chemistry, and analysis of circulating levels of cytokines/chemokines are detailed in the Supplementary Methods.

Histopathology and Immunohistochemistry

Necropsy was performed on all subjects. Tissue samples of all major organs were collected for histopathologic and immunohistochemical (IHC) examination, as outlined in the Supplementary Methods.

Nanostring Sample Preparation

Methods describing sample preparation for transcript quantitation are detailed in the Supplementary Methods.

Bioinformatics

Details of the bioinformatic methods used in this study are available in the Supplementary Methods.

Statistical Analysis

Viral load and Bioplex statistical analyses were carried out using GraphPad Prism version 8. Statistical significance for each Bioplex analyte was assessed using Mann-Whitney nonparametric *t*-tests. A multiple hypothesis Benjamini-Huchberg false discovery rate (FDR) corrected *P*-value less than .05 was deemed significant for all messenger RNA (mRNA) expression analyses, unless otherwise stated. ImmQuant data significance was determined using a 2-tailed unpaired *t*-test with Welch's correction and an FDR-adjusted *P*-value less than .1.

RESULTS

Experimental Infection of Cynomolgus Macaques with NiV and HeV and Comparison to AGMs

To assess the potential for cynomolgus macaques to serve as a model for henipavirus infection in humans, we exposed a group of 8 adult monkeys to either NiV_B (n = 3), NiV_M, (n = 3), or HeV (n = 2). All animals were infected with a total dose of ~ 5.0×10^5 plaque-forming units (PFU) of each respective henipavirus delivered through intranasal and intratracheal inoculation routes (dose divided equally by route). Macaques infected with NiV_B all developed a mild, self-limiting pulmonary illness 5–7 days post infection (dpi), whereas those infected with NiV_M or HeV remained largely asymptomatic (Table 1). Changes in blood cell populations and serum biochemistry in macaques were similar to those observed during henipavirus infection of AGMs (Supplementary Tables 1–3). In contrast to AGMs, which usually succumb to henipavirus infection within 5–10 days after exposure, all 8 infected macaques survived infection to the study's endpoint. All 8 macaques seroconverted and achieved serum neutralization titers comparable to those of AGMs vaccinated against henipavirus infection [20, 24] (Supplementary Table 4).

Lethal henipavirus infection in AGMs typically results in a predictable constellation of gross pathological lesions, which include pleural effusion with fibrinous exudates, necrohemorrhagic interstitial pneumonia, lymphadenomegaly, and congestion in the liver, spleen, and meninges [17, 18, 21–23, 25, 26]. In contrast, necropsies performed on all henipavirus-challenged

Table 1. Clinical Description and Outcome of Cynomolgus Macaques Challenged with NiV_B, NiV_M, and HeV

Subject no.	Sex	Virus	Challenge Dose (PFU)	Clinical Illness	Clinical Pathology	Reference
CYNO-1 (C41446)	M	Bangladesh	~5.0×10^5	Pulmonary edema (d5), lymphadenitis (d5), abdominal breathing (d6-8), fever (d7). Animal survived to study's endpoint (d28).	Lymphopenia (d7); thrombocytopenia (d7,10); leukocytosis (d10,15); reactive thrombocytosis (d15); lymphocytosis (d10); monocytosis (d10); granulocytosis (d5,7,10,15,28); hypoalbuminemia (d15); > 2-fold ↑ in AST (d7); > 8-fold ↑ in CRP (d15)	Unpublished
CYNO-2 (C42728)	M	Bangladesh	~5.0×10^5	Pulmonary edema (d5-7), abdominal breathing (d6,7). Animal survived to study's endpoint (d28).	Lymphopenia (d7); reactive thrombocytosis (d15); lymphocytosis (d15)	Unpublished
CYNO-3 (C40195)	M	Bangladesh	~5.0×10^5	Pulmonary edema (d7), fever (d7), abdominal breathing (d7-8). Animal survived to study's endpoint (d28).	Lymphopenia (d3); thrombocytopenia (d7); monocytopenia (d15); granulocytopenia (d7,10); monocytosis (d10); hypoalbuminemia (d10); > 18-fold ↑ in CRP (d7)	Unpublished
CYNO-4 (C42729)	M	Malaysia	~5.0×10^5	None. Animal survived to study's endpoint (d28).	Monocytopenia (d1,28); granulocytopenia (d1,3,28); leukocytosis (d15); monocytosis (d10); granulocytosis (d15); hypoalbuminemia (d15); > 35% ↓ in CRE (d15); > 19-fold ↑ in CRP (d7)	Unpublished
CYNO-5 (C17438)	M	Malaysia	~5.0×10^5	None. Animal survived to study's endpoint (d28).	Monocytopenia (d1,15,28); granulocytopenia (d3,28); > 2-fold ↑ in ALP (d15); > 8-fold ↑ in CRP (d15)	Unpublished
CYNO-6 (C40693)	M	Malaysia	~5.0×10^5	None. Animal survived to study's endpoint (d28).	Lymphopenia (d5,7); thrombocytopenia (d7); monocytopenia (d5); granulocytopenia (d10); hypoamylasemia (d7); > 8-fold ↑ in CRP (d7)	Unpublished
CYNO-7 (C40541)	M	Hendra	~5.0×10^5	Agitation (d6), increased aggressiveness (d6). Animal survived to study's endpoint (d28).	Lymphopenia (d7); granulocytopenia (d28); granulocytosis (d7); > 40% ↓ in CRE (d5,7)	Unpublished
CYNO-8 (C33314)	M	Hendra	~5.0×10^5	Abdominal breathing (d6). Animal survived to study's endpoint (d28).	Lymphopenia (d7); monocytopenia (d7); granulocytopenia (d15,28); > 2-fold ↑ in ALT (d3); > 2-fold ↑ in AST (d3)	Unpublished

Days after henipavirus challenge are in parentheses, the challenge virus is indicated. Lymphopenia, granulocytopenia, monocytopenia, and thrombocytopenia are defined by a ≥35% drop in numbers of lymphocytes, granulocytes, monocytes, and platelets, respectively. Leukocytosis, monocytosis, and granulocytosis are defined by a 2-fold or greater increase in numbers of white blood cells over base line. Fever is defined as a temperature more than 2.5 °F over baseline, or at least 1.5 °F over baseline and ≥103.5 °F. Hypothermia is defined as a temperature ≤3.5 °F below baseline. Hyperglycemia is defined as a 2-fold or greater increase in levels of glucose. Hypoalbuminemia is defined by a ≥25% decrease in levels of albumin. Hypoproteinemia is defined by a ≥25% decrease in levels of total protein. Hypoamylasemia is defined by a ≥25% decrease in levels of serum amylase. Abbreviations: ALP, alkaline phosphatise; ALT, alanine aminotransferase; AST, aspartate aminotransferase; CRE, creatinine; CRP, C-reactive protein; Hct, hematocrit; Hgb, hemoglobin.

cynomolgus macaques at 28 dpi revealed no evidence of significant lesions that had gone on to resolve. Histopathological and immunohistochemical analysis of formalin-fixed tissues was similarly unremarkable (Supplementary Figure 1), with all NiV_M- and 2/3 NiV_B-infected macaques showing minimal pulmonary edema, and occasionally mild lymphoplasmacytic infiltration of the interstitial space in the kidneys and microvacuolarization of hepatocytes (data not shown). With the sole exception of Cyno-2, which exhibited a focal cluster of neurons within the brainstem with cytoplasmic immunolabeling (Supplementary Figure 1F), none of the macaques displayed immunolabeling for NiV or HeV N protein in any of the tissues analyzed.

Determination of Henipavirus Viral Load and Tissue Tropism

We assessed levels of circulating viremia for each infection group through reverse transcription quantitative polymerase chain reaction (RT-qPCR) amplification of viral genomic RNA (vRNA) and compared these to historical AGM controls. Along with blood draws, swabs were obtained from nasal, oral, and rectal mucosa on procedure days (Supplementary Tables 5,6), with vRNA being present in some or all of the swabs from all of the animals beginning several days post challenge (Figure 1). With the exception of NiV_B-infected macaques, which exhibited significantly lower peak viremia levels than AGMs, we saw no significant difference in peak viral loads in the blood of macaques versus that of AGMs (Supplementary Figure 2A). Similarly, there was no difference between macaques and AGMs in the day on which peak viremia was detected nor the day of earliest detection, whether animals from all 3 virus infections were grouped (Supplementary Figures 2B,C) or analyzed separately (data not shown).

We performed RT-qPCR on RNA from selected tissues harvested from macaques at the study's endpoint (28 dpi), as well as

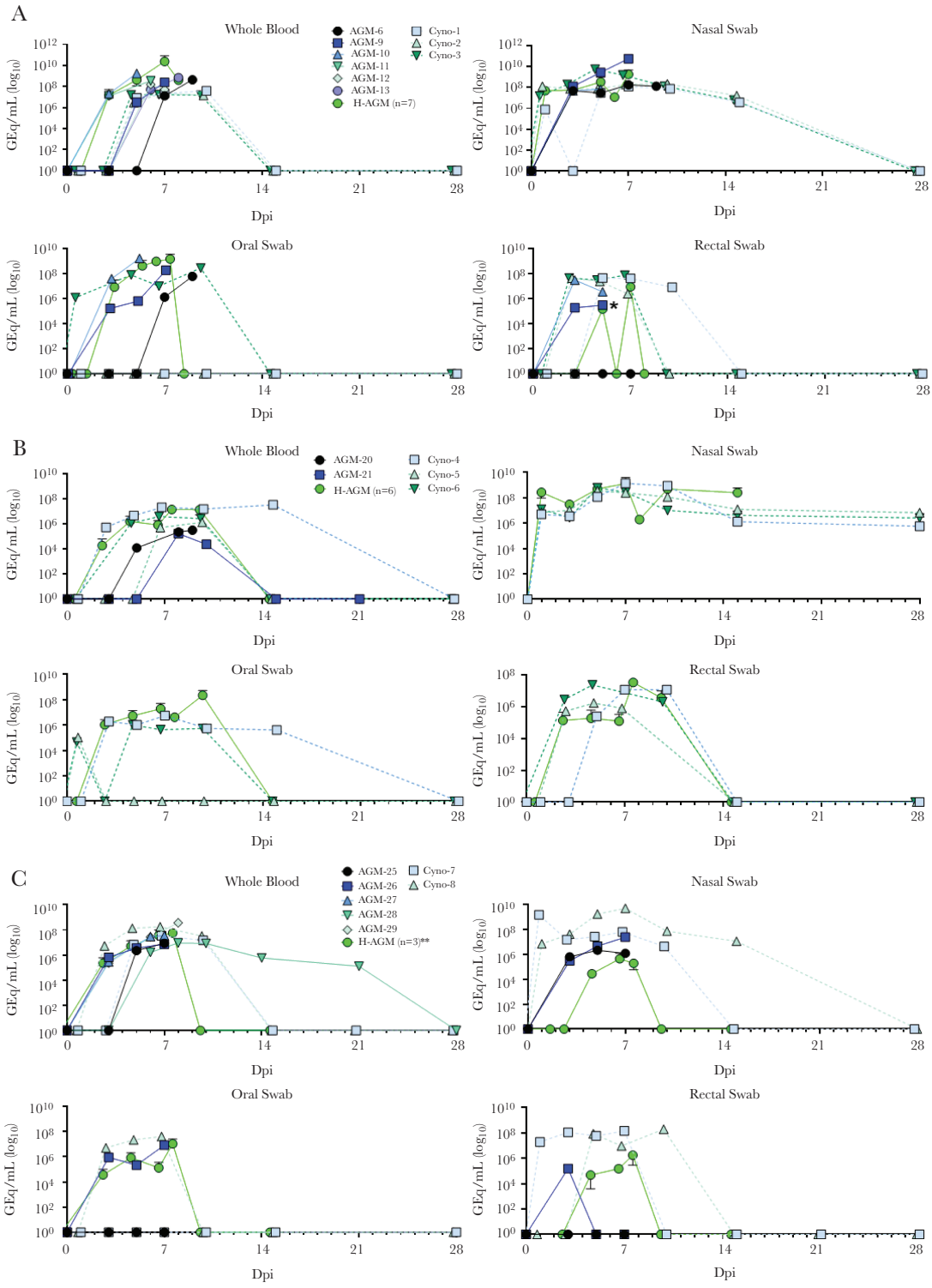

Figure 1. Detection of henipavirus vRNA in blood and mucosa from infected cynomolgus macaques and AGMs. Henipavirus vRNA was detected from whole blood, as well as oral, nasal, and rectal swabs at specific time points during the course of infection using species-specific RT-qPCR primer and probe sets (detailed in Supplemental Methods). For all graphs, solid lines denote AGMs, and dashed lines denote cynomolgus macaques. (*A*), Detection of NiV_B vRNA; (*B*), detection of NiV_M vRNA; (*C*), detection of HeV vRNA. For all graphs, cynomolgus macaques and unpublished AGM controls are plotted individually as the mean of 2 RT-qPCR technical replicates, while the mean value for all previously published historical control AGMs at each timepoint ± SD is shown ("H-AGM"; due to log axis, SD bars extending below 0 cannot be plotted). For the purposes of plotting data on a log scale, samples too low to quantify are plotted as 1 (10^0). Due to differences in sampling schedules between studies, grouped historical controls do not always have the same population size (n) at each timepoint. * The 5 dpi datapoint for subject AGM-9 in the "Rectal Swab" subpanel of (*A*) was the last timepoint for which RNA was available for analysis; RNA from the subsequent time point (7 dpi) was lost during extraction. **Historical control AGM-24 had undetectable quantities of HeV RNA in whole blood and mucosal swabs at all time points assayed. Abbreviations: AGM, African green monkey; HeV, Hendra virus; NiV_B, Nipah virus Bangladesh; NiV_M, Nipah virus Malaysia; RT-qPCR, reverse transcription quantitative polymerase chain reaction; SD, standard deviation.

from historical AGM controls from unpublished studies. AGMs infected with either NiV_B, NiV_M, or HeV all exhibited vRNA titers ranging from ~ 10^5 to10^{12} genome equivalents (GEq) in most assayed tissues (Supplementary Figure 3A–C). In contrast, detection of vRNA in macaques was restricted to lymphoid tissue (Supplementary Figure 3D), and 2 animals, Cyno-3 and Cyno-5, had no vRNA in any tissues analyzed.

Circulating Cytokine/Chemokine Profiles of Henipavirus-Infected Cynomolgus Macaques and Comparison to AGMs

We assessed levels of circulating cytokines and chemokines in the sera of macaques and from archived sera from previously published and unpublished henipavirus-infected AGM control animals. In both species, most analytes remained unchanged or varied between individual animals in response to infection. We selected 8 of the most highly represented analytes for comparative analysis between species. Analyte values from early (3 dpi) or late (7–8 dpi or terminal) infection time points were pooled by species, irrespective of challenge virus or clinical outcome (Supplementary Figure 4A). Interferon γ (IFN-γ) and interleukin (IL)-15 expression was significantly higher in macaques at the early time point, though the higher mean expression of IFN-γ in macaques was strongly influenced by a single animal. Significantly lower IL-4 expression was noted in macaques at the late time point. Monocyte chemoattractant protein-1 (MCP-1) and IL-8 both differed significantly between species early and late in the disease course. In contrast, when only comparing AGMs to each other based on clinical outcome (survivor vs. fatal), none of the analytes showed significant differences between species (Supplementary Figure 4B).

Targeted Transcriptome Profiling of AGMs and Macaques

To further identify immune correlates associated with protection against henipavirus disease, we utilized a targeted transcriptome profiling approach to compare the host immune response in AGMs and cynomolgus macaques. RNA extracted from whole blood from each subject was hybridized with Nanostring NHPV2_Immunology reporter and capture probe sets, and RNA-probe set complexes were processed and imaged on an nCounter® SPRINT Profiler.

We first evaluated the overall relatedness between sample populations by conducting principal component analysis (PCA). Distinct separation of individual AGM and macaque samples indicated robust species-specific differences (Figure 2A). Moreover, disposition, or survivor versus fatal outcome, accounted for the majority of transcriptional changes in the data set. This observation was not altogether surprising given that most subjects in the survivor group were macaques. Additionally, time-dependent expression patterns were evident at baseline (0 dpi), early (3 dpi), and late (7–8 dpi or terminal) time points in the disease course. Accordingly, samples were segregated by early and late disease as was done for cytokine expression comparisons. Samples filtered by challenge virus exhibited minimal dimensional separation, indicating the host response to NiV_B, NiV_M, or HeV manifests similarly in each species. A global scaled heat map depicting unsupervised clustering of the normalized data demonstrated comparable results (Figure 2B).

Samples were segregated by NHP species and disposition to evaluate differential expression, as these groups were deemed the most relevant in terms of global transcriptional changes. Transcriptional profiling by species indicated macaques expressed a higher number of transcripts enriching to adaptive immunity (*FCGR2B*, *LILRB1*, *LILRB2*, *GNLY*) (Figure 3A). Downregulated transcripts in macaques were associated with complement signaling (*C5*, *CD55*, *C4BPA*), apoptosis (*HMGB1*, *AKT3*, *BCL2L1*, *CLU*), granule release (*GZMK*), hematopoiesis (*IL11RA*), and extracellular matrix reorganization (*CEACAM8*) [30–32]. Repression of many of these mRNAs (*C5*, *C4BPA*, *CLU*, *GZMK*, *IL11RA*, *CEACAM8*) was sustained at late in the disease. Besides these changes, we also observed decreased expression of *CD244*, which encodes a cell surface receptor thought to mediate non-major histocompatibility complex (MHC)-restricted killing by natural killer (NK) cells [33]. Late in the disease, upregulated transcripts in macaques were involved in B-cell antigen presentation (*CD79A*); differentiation of B cells into antibody-secreting plasma cells (*MS4A1*); myeloid cell maturation (*IRF8*); and defensin activity (*DEFA1*) [34–37]. Similarly, grouping by survivors, which pooled common differentially expressed transcripts (DETs) for cynomolgus macaques and the 5 surviving AGMs, indicated increased expression of transcripts involved in adaptive immunity (*SLAMF6*, *FYN*, *SH2D1A*, *CCR5*) compared to fatal AGM subjects. Additionally, transcripts relating to T-cell function, differentiation, and activation were upregulated in survivors (Figure 3B). Specifically, we observed a greater $\log_2$-fold change for T-cell receptor (TCR)-associated transcripts (*CD3G*, *CD3D*, *CD3E*), T-cell coreceptor signaling molecules (*CD8A*, *LCK*), and the master transcriptional regulator for T helper 1 (Th1) cells, *TBX21* [38]. In contrast, mRNAs affiliated with interferon (IFN) signaling were repressed in survivors (*MX2*, *GBP1*, *JAK2*, *IL18*, *CXCL10*). In late disease, no DETs were noted other than decreased expression of *IL1R2*, a decoy receptor in the IL-1 family that inhibits activity of its ligands, IL-1α and IL-1β [39]. Thus, survivor transcriptional signatures correlated with Th1 differentiation and activation of adaptive responses, whereas poor prognosis was associated with innate signaling.

To determine canonical signaling pathways associated with survival, we performed IPA-based functional enrichment of DETs. AGMs were segregated by disposition (fatal or survivor), whereas macaques were combined into a single survivor group for this analysis. The AGM survivor group was not displayed at early disease as no significantly enriched pathways were identified at this time point.

All groups shared pathways mapping to IFN, pattern recognition receptor, neuroinflammation, and nitric oxide signaling (Figure 4). Other common upregulated pathways included T-cell exhaustion, Tec kinase signaling, dendritic cell maturation, and

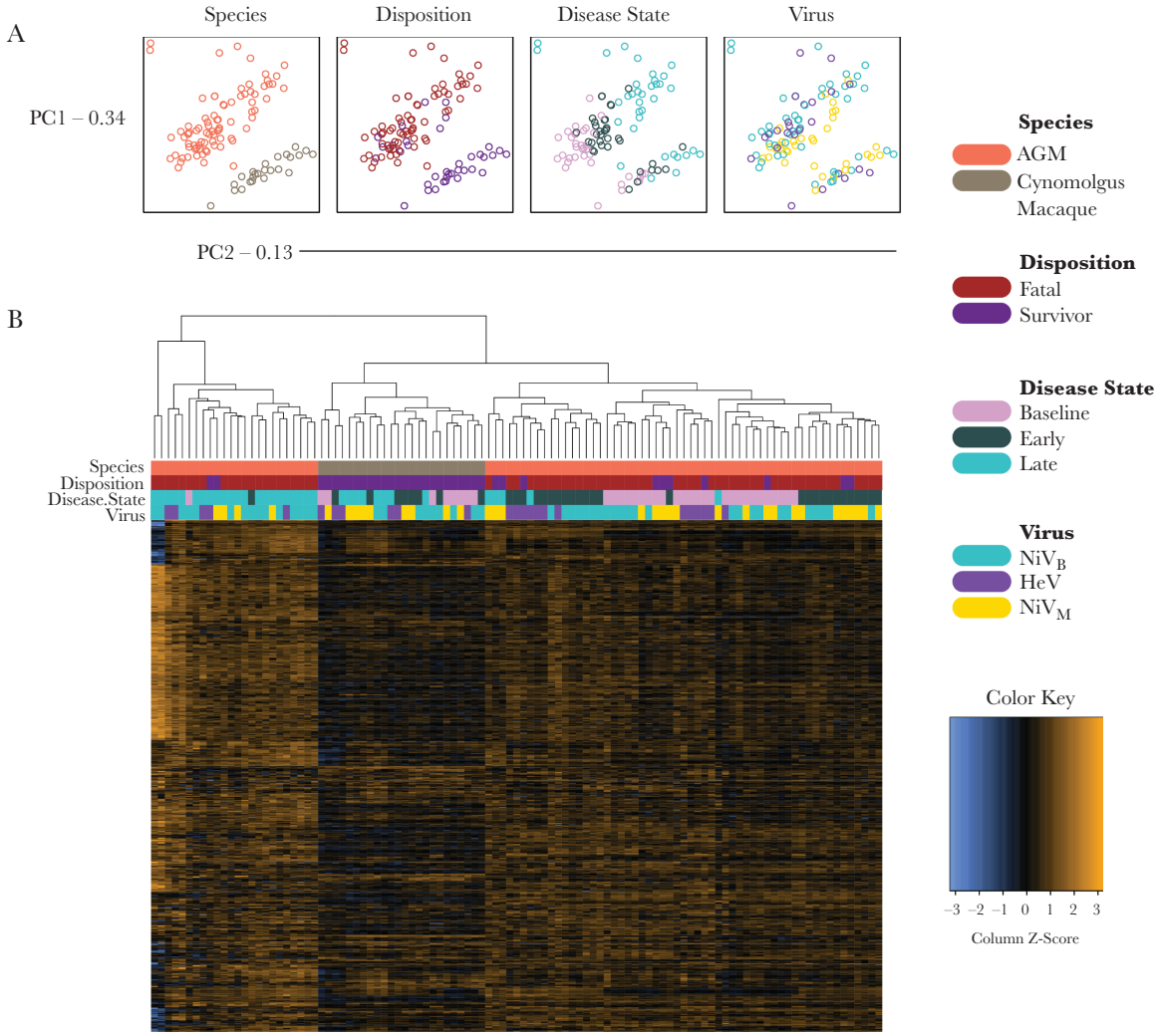

Figure 2. Transcriptional changes grouped by each covariate. (*A*), Principal component analysis of all differentially expressed transcripts at baseline, early, and late disease. Shown are individual samples isolated by species, disposition, disease state, or challenge virus. (*B*), Heat map of normalized data generated via unsupervised clustering. Data were scaled to give all genes equal variance. Orange indicates high expression (z-scores); blue indicates low expression. Baseline (pre-challenge); early disease (3 days post infection); late disease (7 days post infection in survivors, or the terminal time point in fatal subjects). Specific *P*-values for each transcript and comparison are provided in Supplementary Data 1. Abbreviations: AGM, African green monkey; HeV, Hendra virus; NiV$_B$, Nipah virus Bangladesh; NiV$_M$, Nipah virus Malaysia; PC1, principal component 1; PC2, principal component 2.

TREM1 signaling. As with our differential expression analysis, survival correlated with T-cell differentiation. For example, we observed positive z-scores in AGM and macaque survivor groups for the Th1 pathway and Jak/Stat signaling at late disease. Th2 and Th17 pathways were also upregulated in macaque survivors at this point. Additionally, NF-κβ signaling was enhanced in both survivor groups. Conversely, transcripts associated with T-cell activation and differentiation, for example, IL-2 signaling, Th1 and Th2 pathways, TGF-β, IL-23, and CD40 canonical pathways, were downregulated in the AGM fatal group at this time point. Instead, these animals expressed transcripts mapping to TLR, MAPK, PD-1, complement, and LPS/IL-1-related pathways. These data suggest that henipavirus disease is associated with prolonged innate signaling, complement activation, and suppression of T-cell responses.

To further capture shifts in circulating immune cell populations, we used nSolver cell type profiling and ImmQuant DCQ (IRIS database). In line with our differential expression analysis and IPA results, the nSolver approach indicated DETs in the fatal versus survivor data set were associated with increased frequencies of B cells and Th1 cells (Figure 5A). B-cell-type quantities were also higher in macaques. In contrast, frequencies of mast cells, NK cells, and exhausted CD8$^+$ T cells were predicted to decrease in AGM survivor and macaque groups. To cross-validate our results, ImmQuant DCQ was used to calculate relative changes at early and late disease. In late disease, we observed statistically significant cell type abundances of dendritic cells, monocytes, and resting neutrophils in the fatal group. In agreement with our nSolver estimations, increased B-cell memory immunoglobulin M (IgM) and plasma cell

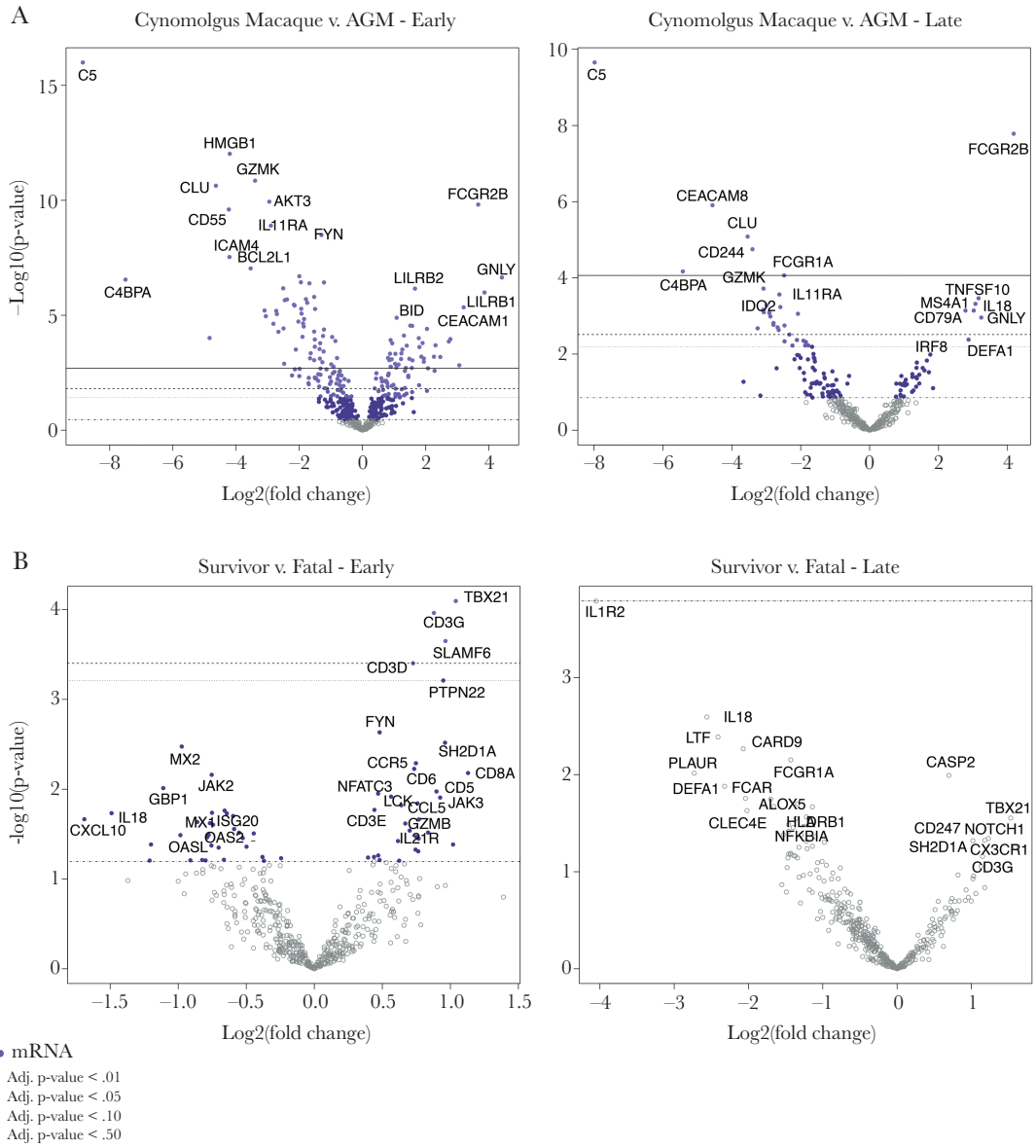

Figure 3. Volcano plots indicating transcriptional changes for disposition and species covariates. Displayed are -log10 (*P*-values) and log2-fold changes for each mRNA target segregated by (*A*) disposition (survivor vs. fatal subjects) or (*B*) species (cynomolgus macaque vs. AGM). Horizontal lines within the plot indicate adjusted *P*-value thresholds. Targets highlighted in blue indicate adjusted *P*-values <.10. Abbreviations: AGM, African green monkey; mRNA, messenger RNA.

quantities were found in survivors (Figure 5B). In early disease, NK cells and CD4 T cells were predicted to increase in the fatal group, and again frequencies of B cell memory IgM and plasma cell quantities were higher in survivors. Furthermore, plasma cells were detected in the macaque group in early and late disease time points (Figure 5C). In the AGM group, DCQ profiling indicated expansion of dendritic cell, late-differentiated monocyte, and Th2 cell populations.

DISCUSSION

The bioweapon potential of NiV and HeV, along with the increased frequency of outbreaks (particularly for NiV_B), makes development and approval of vaccines and therapeutics for henipaviruses of critical importance. These efforts are complicated by the restriction of research involving infectious HeV and NiV to BSL-4 laboratories. Moreover, the unpredictable nature of outbreaks makes conducting efficacy trials of vaccines and therapeutics in humans difficult to plan and execute. Given these limitations, it is likely that any approval of a henipavirus vaccine or therapeutic will have to rely on data generated in animal models under the US Food and Drug Administration Animal Rule. Although AGMs have proven to be a valuable species for accurately modeling henipavirus disease seen in humans, development of an equivalent model in

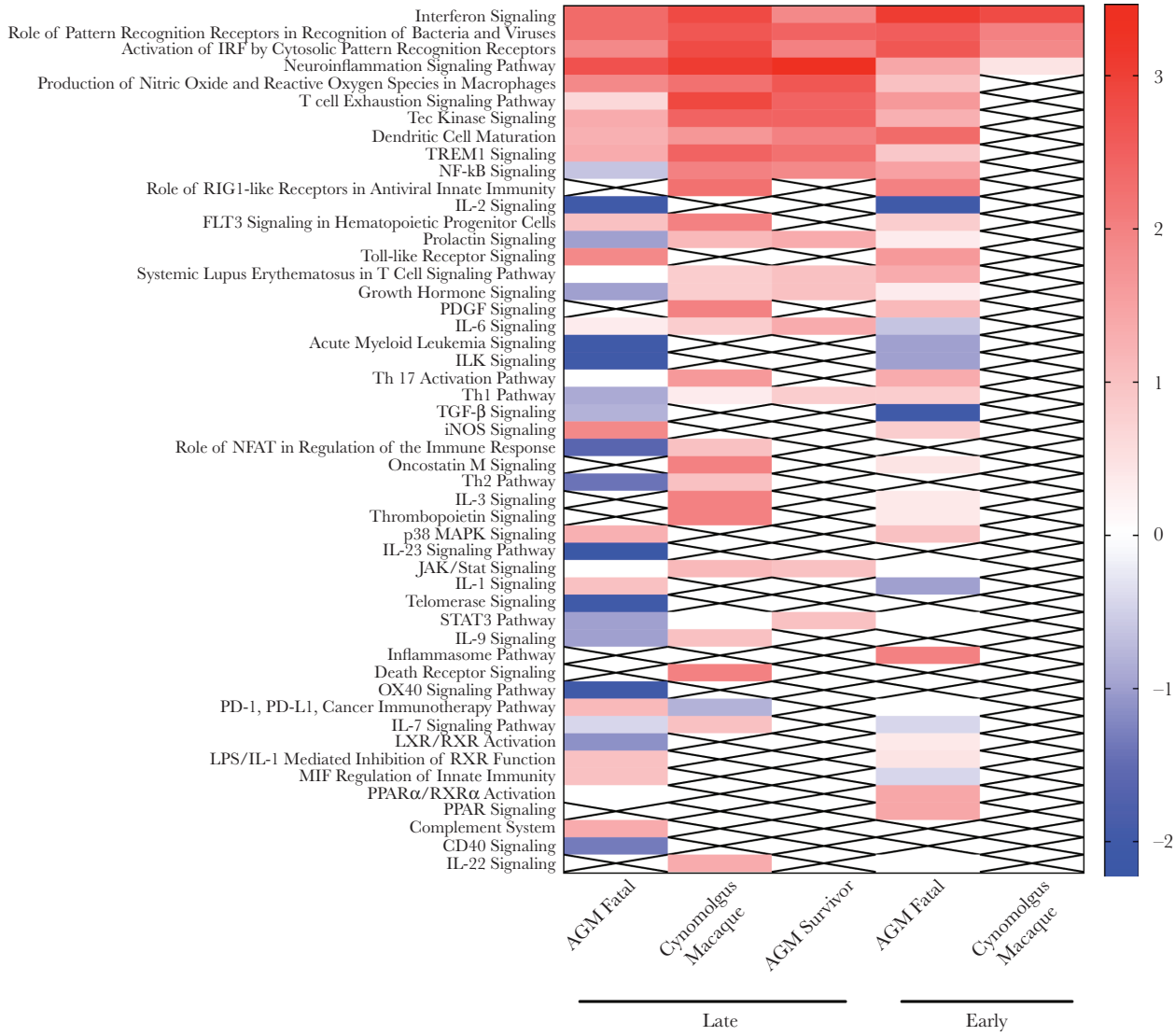

Figure 4. Heatmap demonstrating the most highly upregulated and downregulated canonical pathways at each disease stage. Only differentially expressed transcripts with an FDR-corrected *P*-value of less than .05 were enriched with ingenuity pathway analysis (Qiagen). The data were normalized against a day 0 pre-challenge baseline for each NHP subject at early and late disease. Red indicates high expression (z-scores); blue indicates low expression. "X's" indicate insufficient transcripts mapping to the indicated pathway. Abbreviations: AGM, African green monkey; FDR, false discovery rate; NHP, nonhuman primate.

a well-characterized NHP species would be of benefit for numerous practical and logistical reasons.

In the present study, we assessed the potential of cynomolgus macaques as surrogates to AGMs for modeling henipavirus infection in humans. In contrast to the severe and usually fatal disease seen in AGMs, infection with NiV_B, NiV_M, or HeV resulted in only mild or asymptomatic infection in macaques. This surprising inability of all 3 henipaviruses to cause severe clinical disease in macaques similar to that seen in AGMs, with the exception of NiV_B, which produced markedly lower levels of vRNA in the blood than in AGMs.

In an effort to identify correlates of protection from lethal henipavirus-induced disease, we profiled serum cytokine/chemokine levels as well as immune transcript expression at early and late time points in the disease course and made comparisons between species and clinical outcome. Several cytokines showed significant differential abundance in AGMs and macaques at early and/or late time points. Specifically, modest levels of IL-15 and IL-8 were found in macaques versus AGMs but not in AGMs surviving henipavirus infection compared to those that succumbed to disease. However, these cytokines were more abundant in late disease in AGMs, along with other pro- and anti-inflammatory mediators. Conversely, IL-4 and MCP-1 concentrations were higher in AGMs than macaques. IFN-γ and IL-4 are pleiotropic cytokines that play opposing roles in T cell development: both act in positive-feedback loops to stimulate differentiation of naive $CD4^+$ T cells into Th1 and Th2 cells, respectively, while also suppressing differentiation of the

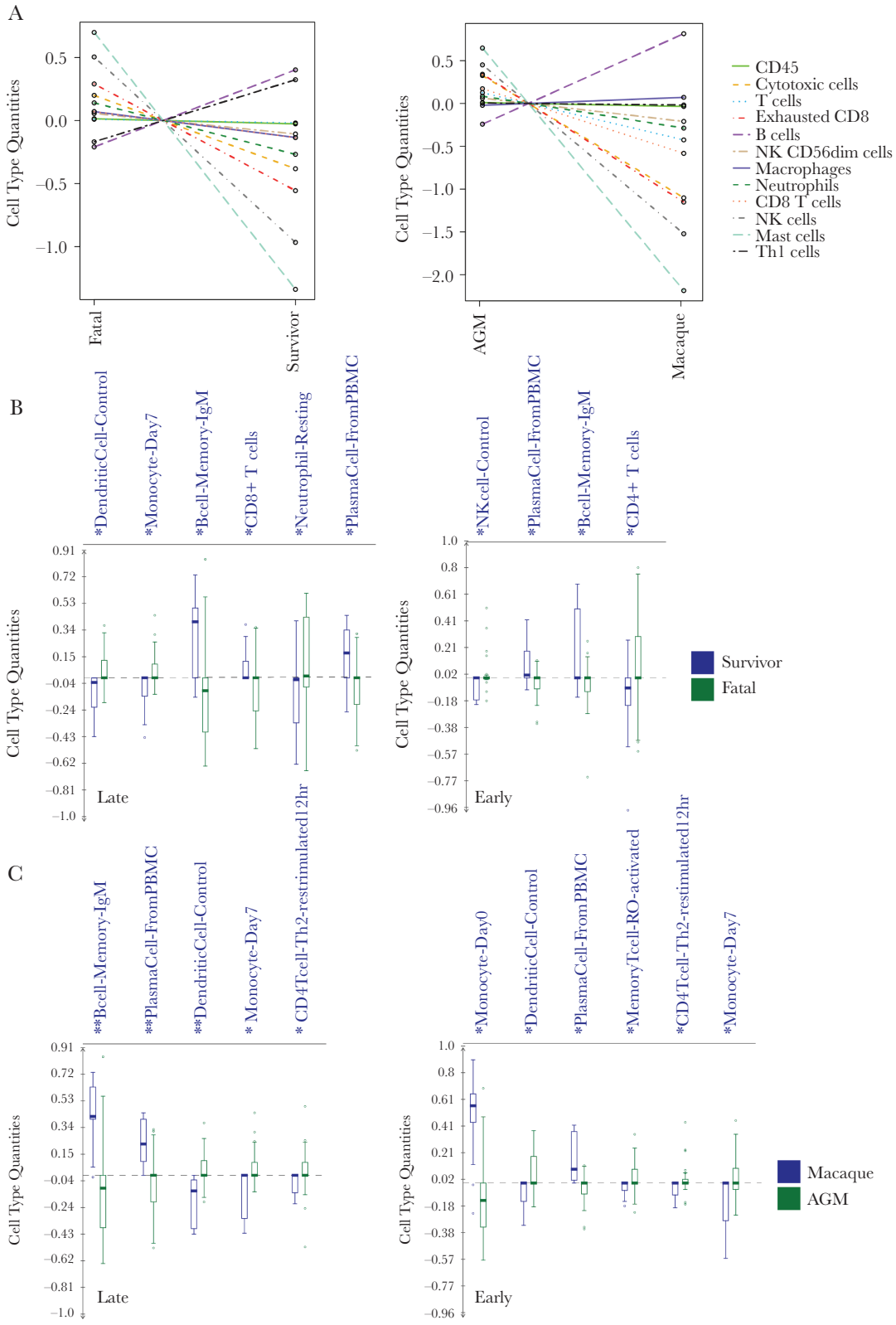

Figure 5. Immune cell type profiling of disposition and species covariates. (*A*), Overall respective cell-type quantities for disposition (left) and species (right) covariates determined using the Nanostring nSolver Advanced Analysis plug-in. Baseline (pre-challenge); early disease (3 days post infection); late disease (7 days post infection in survivors, or the terminal time point in fatal subjects). (*B*), Bar graphs of immune-cell type quantities at late (left) and early (right) disease. Frequencies were predicted using ImmQuant software and the IRIS database. Mean and SD shown. Significance was determined using unpaired 2-tailed *t*-test with Welch's correction; *, *P*-value <.05; **, *P*-value <.01. Abbreviations: AGM, African green monkey; SD, standard deviation.

reciprocal cell type [40]. IL-15 plays roles in mediating the pro-inflammatory response and memory T-cell generation, among many others [41]. IL-8 is secreted by macrophages, epithelial cells, endothelial cells, and other cells types to induce chemotaxis of granulocytes (e.g., neutrophils) toward sites of infection. The stark difference between MCP-1 abundance in AGMs and macaques is of particular interest because of its primary role as a monocyte recruitment chemoattractant. Specifically, in addition to other leukocytes, monocytes, which do not support NiV replication, can bind the virus to the cell surface and facilitate trans-infection both in vitro and in vivo, allowing for spread of the virus via the hematogenous route [42, 43]. Moreover, dendritic cells, which can support low levels of NiV replication, are differentiated in the presence of MCP-1 [42–44]. Thus, the relative low abundance of MCP-1 in macaques versus AGMs may play a protective role in these animals by limiting the availability of cells for trans-endothelial dissemination. High levels of IL-8 and MCP-1 correspond with fatal outcome in other NHP studies involving NiV [23].

To further investigate species-specific differences in host immune responses that contribute to henipavirus disease, we utilized a targeted transcriptome profiling approach, a method previously utilized for Ebola virus infection studies in NHPs [45]. Clustering by IPA indicated species and disposition were the primary parameters that accounted for the majority of gene expression changes. Our analysis revealed increased expression of adaptive immunity pathways and related transcripts in both macaque and survivor datasets. Specifically, in silico analysis using nSolver and ImmQuant showed recruitment of Th1 cells, plasma cells, cytotoxic $CD8^+$ T cells, and IgM^+ B cells. In fatal and AGM subjects, dysregulation of complement and IFN signaling was a notable finding. Conversely, predicted granulocyte expansion, complement dysregulation, and prolonged innate signaling contributed to fatal disease. Skewing of T-helper cells toward the Th1 subtype was previously demonstrated in AGMs surviving NiV_M-infection [22, 46]. Our data suggest that macaques and surviving AGMs promote Th1 differentiation, at least in part by maintaining low levels of pro-Th2/anti-Th1 IL-4 and higher levels of pro-Th1/anti-Th2 IFN-γ early in infection. Other cell subsets (NK cells, NK T cells) that lack antigen specificity may contribute to the high levels of IFN-γ seen in fatal AGM subjects at late disease [47]. Secretion of IFN-γ may instead contribute to inflammation, as these cells are unable to specifically recognize virally infected cells [48]. Alternatively, Th1 cells may be recruited into tissues in survivors, or these cells may be recruited too late in disease to adequately combat infection in fatal subjects.

Given the strong correlation between cellular and humoral immunity on intra- and interspecies specific disease and survival outcomes to henipavirus infection, the ability of henipaviruses to replicate relatively benignly in macaques to levels that cause lethal disease in AGMs may seem counterintuitive. Similarly, AGMs and sooty mangabeys sustain high viral loads of simian immunodeficiency virus (SIV) and do not progress to AIDS, whereas rhesus macaques follow the disease progression seen with human immunodeficiency virus (HIV) in humans [48]. To address these seemingly paradoxical observations, Palesch and colleagues recently conducted a survey of the sooty mangabey transcriptome and found substantial sequence divergence in several immune genes compared to AIDS-susceptible human and macaque orthologs, including TLR-4, which is thought to cause SIV-induced chronic inflammation and eventual immune collapse [49]. Likewise, genetic or epigenetic differences between cynomolgus macaques, humans, and AGMs may also contribute to differences in host immune responses, and are avenues of further research. Indeed, the present study provides an interesting observation that cynomolgus macaques native to Southeast Asia, where pathogenic henipaviruses are endemic, respond to infection with minimal pathological outcome, whereas the AGM presents with severe disease following infection by NiV and HeV, viruses not known to be present in the natural geographic range of AGMs. Our data identify potentially promising host pathways for rational design of henipavirus therapeutics. Future studies assessing Th1 adjuvants as a postexposure intervention to enhance protection is but one approach that may have utility in combating henipavirus infection.

Supplementary Data

Supplementary materials are available at *The Journal of Infectious Diseases online*. Consisting of data provided by the authors to benefit the reader, the posted materials are not copyedited and are the sole responsibility of the authors, so questions or comments should be addressed to the corresponding author.

Notes

Acknowledgments. The authors would like to thank the UTMB Animal Resource Center for husbandry support of laboratory animals and Natalie Dobias for expert histology and immunohistochemistry support.

Funding. This study was supported in part by the Department of Health and Human Services, National Institutes of Health, grants AI082121 to T. W. G. and in part by the Department of Microbiology and Immunology, University of Texas Medical Branch at Galveston, Galveston, TX, to T. W. G. Operations support of the Galveston National Laboratory was supported by NIAID/NIH grant UC7AI094660.

Availability of data and materials. The data sets used and/or analyzed during the current study are available from the corresponding author on reasonable request.

Authors' contributions. C. C. B. and T. W. G. conceived and designed the study. J. B. G. and T. W. G. performed the henipavirus challenge experiments. J. B. G., D. J. D., R. W. C., C. E. M., and T. W. G. performed animal procedures and clinical

observations. J. B. G., K. N. A., V. B., and D. J. D. performed the clinical pathology assays. J. B. G. and V. B. performed the henipavirus infectivity assays. K. N. A. performed the PCR and multiplex assays. C. W. performed the Nanostring assays. A. N. P., C. W., J. B. G., K. N. A., V. B., R. W. C., K. A. F., C. C. B., and T. W. G. analyzed the data. K. A. F. performed gross pathologic, histologic, and immunohistochemical analysis of the data. A. N. P., C. W., K. A. F, C. C. B., and T. W. G. wrote the article. R. W. C. edited the article. All authors had access to all of the data and approved the final version of the article.

Consent for publication. Not applicable.

Potential conflicts of interest. All authors declare that they have no conflicts of interest.

All authors have submitted the ICMJE Form for Disclosure of Potential Conflicts of Interest. Conflicts that the editors consider relevant to the content of the manuscript have been disclosed.

Presentation history: None.

References

1. Sharma V, Kaushik S, Kumar R, Yadav JP, Kaushik S. Emerging trends of Nipah virus: a review. Rev Med Virol **2019**; 29:e2010.
2. Weingartl H. Hendra and Nipah viruses: pathogenesis, animal models and recent breakthroughs in vaccination. Vaccine: Development and Therapy **2015**; 5:59–74.
3. Wong KT, Ong KC. Pathology of acute henipavirus infection in humans and animals. Patholog Res Int **2011**; 2011:567248.
4. Clayton BA, Wang LF, Marsh GA. Henipaviruses: an updated review focusing on the pteropid reservoir and features of transmission. Zoonoses Public Health **2013**; 60:69–83.
5. Field H, de Jong C, Melville D, et al. Hendra virus infection dynamics in Australian fruit bats. PLoS One **2011**; 6:e28678.
6. Chua KB, Bellini WJ, Rota PA, et al. Nipah virus: a recently emergent deadly paramyxovirus. Science **2000**; 288:1432–5.
7. Harcourt BH, Lowe L, Tamin A, et al. Genetic characterization of Nipah virus, Bangladesh, 2004. Emerg Infect Dis **2005**; 11:1594–7.
8. Ang BSP, Lim TCC, Wang L. Nipah virus infection. J Clin Microbiol **2018**; 56:1–10.
9. Ching PK, de los Reyes VC, Sucaldito MN, et al. Outbreak of henipavirus infection, Philippines, 2014. Emerg Infect Dis **2015**; 21:328–31.
10. Lo MK, Lowe L, Hummel KB, et al. Characterization of Nipah virus from outbreaks in Bangladesh, 2008–2010. Emerg Infect Dis **2012**; 18:248–55.
11. Arunkumar G, Chandni R, Mourya DT, et al. Outbreak investigation of Nipah virus disease in Kerala, India, 2018. J Infect Dis **2019**; 219:1867–78.
12. Gurley ES, Montgomery JM, Hossain MJ, et al. Person-to-person transmission of Nipah virus in a Bangladeshi community. Emerg Infect Dis **2007**; 13:1031–7.
13. Luby SP, Gurley ES, Hossain MJ. Transmission of human infection with Nipah virus. Clin Infect Dis **2009**; 49:1743–8.
14. Nikolay B, Salje H, Hossain MJ, et al. Transmission of Nipah virus - 14 years of investigations in Bangladesh. N Engl J Med **2019**; 380:1804–14.
15. Allio T. Product development under FDA's animal rule: understanding FDA's expectations and potential implications for traditional development programs. Ther Innov Regul Sci **2016**; 50:660–70.
16. Geisbert TW, Feldmann H, Broder CC. Animal challenge models of henipavirus infection and pathogenesis. Curr Top Microbiol Immunol **2012**; 359:153–77.
17. Geisbert TW, Daddario-DiCaprio KM, Hickey AC, et al. Development of an acute and highly pathogenic nonhuman primate model of Nipah virus infection. PLoS One **2010**; 5:e10690.
18. Rockx B, Bossart KN, Feldmann F, et al. A novel model of lethal Hendra virus infection in African green monkeys and the effectiveness of ribavirin treatment. J Virol **2010**; 84:9831–9.
19. Geisbert TW, Mire CE, Geisbert JB, et al. Therapeutic treatment of Nipah virus infection in non-human primates with a neutralizing human monoclonal antibody. Sci Transl Med **2014**; 6:242ra82.
20. Mire CE, Geisbert JB, Agans KN, et al. A recombinant Hendra virus G glycoprotein subunit vaccine protects nonhuman primates against Hendra virus challenge. J Virol **2014**; 88:4624–31.
21. Mire CE, Satterfield BA, Geisbert JB, et al. Pathogenic differences between Nipah virus Bangladesh and Malaysia strains in primates: implications for antibody therapy. Sci Rep **2016**; 6:30916.
22. Cong Y, Lentz MR, Lara A, et al. Loss in lung volume and changes in the immune response demonstrate disease progression in African green monkeys infected by small-particle aerosol and intratracheal exposure to Nipah virus. PLoS Negl Trop Dis **2017**; 11:e0005532.
23. Hammoud DA, Lentz MR, Lara A, et al. Aerosol exposure to intermediate size Nipah virus particles induces neurological disease in African green monkeys. PLoS Negl Trop Dis **2018**; 12:e0006978.
24. Mire CE, Geisbert JB, Agans KN, et al. Use of single-injection recombinant vesicular stomatitis virus vaccine to protect nonhuman primates against lethal Nipah virus disease. Emerg Infect Dis **2019**; 25:1144–52.
25. Geisbert JB, Borisevich V, Prasad AN, et al. An intranasal exposure model of lethal Nipah virus infection in African green monkeys. J Infect Dis **2019**;221(S4):S414–8.

26. Prasad AN, Agans KN, Sivasubramani SK, et al. A lethal aerosol exposure model of Nipah virus strain Bangladesh in African green monkeys. J Infect Dis **2020**;221(S4):S431–5.
27. Lankau EW, Turner PV, Mullan RJ, Galland GG. Use of nonhuman primates in research in North America. J Am Assoc Lab Anim Sci **2014**; 53:278–82.
28. Pandrea I, Ribeiro RM, Gautam R, et al. Simian immunodeficiency virus SIVagm dynamics in African green monkeys. J Virol **2008**; 82:3713–24.
29. Brinton MA, Di H, Vatter HA. Simian hemorrhagic fever virus: recent advances. Virus Res **2015**; 202:112–9.
30. Jones SE, Jomary C. Clusterin. Int J Biochem Cell Biol **2002**; 34:427–31.
31. Shi L, Kam CM, Powers JC, Aebersold R, Greenberg AH. Purification of three cytotoxic lymphocyte granule serine proteases that induce apoptosis through distinct substrate and target cell interactions. J Exp Med **1992**; 176:1521–9.
32. Chérel M, Sorel M, Lebeau B, et al. Molecular cloning of two isoforms of a receptor for the human hematopoietic cytokine interleukin-11. Blood **1995**; 86:2534–40.
33. Mathew SO, Rao KK, Kim JR, Bambard ND, Mathew PA. Functional role of human NK cell receptor 2B4 (CD244) isoforms. Eur J Immunol **2009**; 39:1632–41.
34. Gaul BS, Harrison ML, Geahlen RL, Burton RA, Post CB. Substrate recognition by the Lyn protein-tyrosine kinase. NMR structure of the immunoreceptor tyrosine-based activation motif signaling region of the B cell antigen receptor. J Biol Chem **2000**; 275:16174–82.
35. Tedder TF, Streuli M, Schlossman SF, Saito H. Isolation and structure of a cDNA encoding the B1 (CD20) cell-surface antigen of human B lymphocytes. Proc Natl Acad Sci U S A **1988**; 85:208–12.
36. Holtschke T, Löhler J, Kanno Y, et al. Immunodeficiency and chronic myelogenous leukemia-like syndrome in mice with a targeted mutation of the ICSBP gene. Cell **1996**; 87:307–17.
37. Valore EV, Ganz T. Posttranslational processing of defensins in immature human myeloid cells. Blood **1992**; 79:1538–44.
38. Szabo SJ, Kim ST, Costa GL, Zhang X, Fathman CG, Glimcher LH. A novel transcription factor, T-bet, directs Th1 lineage commitment. Cell **2000**; 100:655–69.
39. Lang D, Knop J, Wesche H, et al. The type II IL-1 receptor interacts with the IL-1 receptor accessory protein: a novel mechanism of regulation of IL-1 responsiveness. J Immunol **1998**; 161:6871–7.
40. Luckheeram RV, Zhou R, Verma AD, Xia B. $CD4^+$T cells: differentiation and functions. Clin Dev Immunol **2012**; 2012:925135.
41. Perera PY, Lichy JH, Waldmann TA, Perera LP. The role of interleukin-15 in inflammation and immune responses to infection: implications for its therapeutic use. Microbes Infect **2012**; 14:247–61.
42. Mathieu C, Pohl C, Szecsi J, et al. Nipah virus uses leukocytes for efficient dissemination within a host. J Virol **2011**; 85:7863–71.
43. Tiong V, Shu MH, Wong WF, AbuBakar S, Chang LY. Nipah virus infection of immature dendritic cells increases its transendothelial migration across human brain microvascular endothelial cells. Front Microbiol **2018**; 9:2747.
44. Omata N, Yasutomi M, Yamada A, Iwasaki H, Mayumi M, Ohshima Y. Monocyte chemoattractant protein-1 selectively inhibits the acquisition of CD40 ligand-dependent IL-12-producing capacity of monocyte-derived dendritic cells and modulates Th1 immune response. J Immunol **2002**; 169:4861–6.
45. Speranza E, Altamura LA, Kulcsar K, et al. Comparison of transcriptomic platforms for analysis of whole blood from Ebola-infected cynomolgus macaques. Sci Rep **2017**; 7:14756.
46. Lara A, Cong Y, Jahrling PB, et al. Peripheral immune response in the African green monkey model following Nipah-Malaysia virus exposure by intermediate-size particle aerosol. PLoS Negl Trop Dis **2019**; 13:e0007454.
47. He XS, Draghi M, Mahmood K, et al. T cell-dependent production of IFN-gamma by NK cells in response to influenza A virus. J Clin Invest **2004**; 114:1812–9.
48. Jacquelin B, Mayau V, Targat B, et al. Nonpathogenic SIV infection of African green monkeys induces a strong but rapidly controlled type I IFN response. J Clin Invest **2009**; 119:3544–55.
49. Palesch D, Bosinger SE, Tharp GK, et al. Sooty mangabey genome sequence provides insight into AIDS resistance in a natural SIV host. Nature **2018**; 553:77–81.